Cellular uptake of functionalized carbon nanotubes is independent of functional group and cell type

KOSTAS KOSTARELOS[1]*, LARA LACERDA[1], GIORGIA PASTORIN[3], WEI WU[3], SÉBASTIEN WIECKOWSKI[3], JACQUELINE LUANGSIVILAY[3], SYLVIE GODEFROY[3], DAVIDE PANTAROTTO[2,3], JEAN-PAUL BRIAND[3], SYLVIANE MULLER[3], MAURIZIO PRATO[3]* AND ALBERTO BIANCO[2]*

[1]Nanomedicine Laboratory, Centre for Drug Delivery Research, The School of Pharmacy, University of London, London WC1N 1AX, United Kingdom
[2]CNRS, Institut de Biologie Moléculaire et Cellulaire, Laboratoire d'Immunologie et Chimie Thérapeutiques, 67000 Strasbourg, France
[3]Dipartimento di Scienze Farmaceutiche, Università di Trieste, 34127 Trieste, Italy
*e-mail: kostas.kostarelos@pharmacy.ac.uk; a.bianco@ibmc.u-strasbg.fr; prato@univ.trieste.it

Published online: 28 January 2007; doi:10.1038/nnano.2006.209

The development of nanomaterials for biomedical and biotechnological applications is an area of research that holds great promise and intense interest[1], and carbon-based nanostructures in particular, such as carbon nanotubes (CNTs), are attracting an increasing level of attention[2,3]. One of the key advantages that CNTs offer is the possibility of effectively crossing biological barriers, which would allow their use in the delivery of therapeutically active molecules. Our laboratories have been investigating the use of CNTs in biomedical applications, and in particular as nanovectors for therapeutic agent delivery[4–8]. The interaction between cells and CNTs is a critical issue that will determine any future biological application of such structures. Here we show that various types of functionalized carbon nanotubes (*f*-CNTs) exhibit a capacity to be taken up by a wide range of cells and can intracellularly traffic through different cellular barriers.

Water-soluble *f*-CNTs interact with mammalian cells, leading to their cytoplasmic translocation[5,7]. Ammonium-functionalized cationic nanotubes condense and deliver plasmid DNA (pDNA) intracellularly, leading to enhanced marker gene expression[7,9–11]. Other studies indicate that CNTs coated with proteins[12], polymers[13] and single-stranded DNA[14] also interact with mammalian cells, reporting the intracellular translocation of these macromolecules. Also, an increasing number of reports have studied the toxicological impact and safety profile of carbon nanomaterials[15,16], indicating that a high degree of CNT functionalization leads to a dramatic reduction in toxic effects[17]. However, the fundamental question of whether *f*-CNTs, in the absence of any coating or conjugation with macromolecules, are capable of cell binding, uptake and internalization has not yet been addressed.

The present study is designed to elucidate if *f*-CNTs are capable of interaction with cells and to determine the critical parameters in such interactions. We describe a series of experiments using functionalized single-walled (*f*-SWNTs) and multiwalled (*f*-MWNTs) CNTs with a wide variety of functional groups (Fig. 1). Intrinsically luminescent or fluorescently labelled *f*-CNTs were directly tracked and imaged intracellularly by epifluorescence and confocal laser scanning microscopy (CLSM). The imaging of *f*-CNTs and not their adsorbed macromolecules, as previously reported by other groups[12,18,19], is imperative in order to elucidate their interaction with cellular compartments. Even in studies tracking the intracellular localization of non-functionalized pristine CNTs (pCNTs) solubilized by polymer or single-stranded DNA molecules by the IR spectral characteristics of the pCNT backbone[13,14,20], one should be very cautious when extrapolating conclusions about pCNT–cellular compartment interactions. Indeed, the effect of the macromolecules acting as their solubilizing agent can play a critical role in determining the type of ensuing interactions with cells and the mechanisms of cellular uptake, as has been shown for other polymer-coated nanostructures[21].

The functionalization of SWNTs and MWNTs in this study was mainly performed by using the 1,3-dipolar cycloaddition of azomethine ylides[22,23]. This approach allows insertion of amino functions around the sidewalls and at the tips of the CNTs, which renders the tubes highly soluble in aqueous environments. The amino groups were further modified by covalently linking a variety of small molecules including fluorescent probes[5] and anticancer and antibiotic agents[24,25]. The addition of functional groups was carried out in a modular fashion, gradually increasing the molecular complexity of the groups covalently linked onto the nanotube sidewalls (Fig. 1). Figure 2 shows representative transmission electron microscopy (TEM) images of the functionalized multiwalled *f*-CNTs **1** (Fig. 2b) and **6** (Fig. 2c), compared with the non-functionalized starting material (Fig. 2a). In agreement with other studies that used differently functionalized CNTs (refs 26–28), *f*-CNTs **1** and **2** were found to be intrinsically luminescent in the ultraviolet/visible region[29,30]. Meanwhile, *f*-CNTs **3**–**7** were conjugated with fluorescein isothiocyanate (FITC) to obtain high levels of fluorescence signal.

The interaction between *f*-CNTs and a wide variety of live cells was then studied. All *f*-CNTs were allowed to interact with different cell types as illustrated in Table 1. The conditions were identical, ranging in incubation times from 1 to 4 h at 37 °C in the cell medium. In Table 1, representative images using CLSM

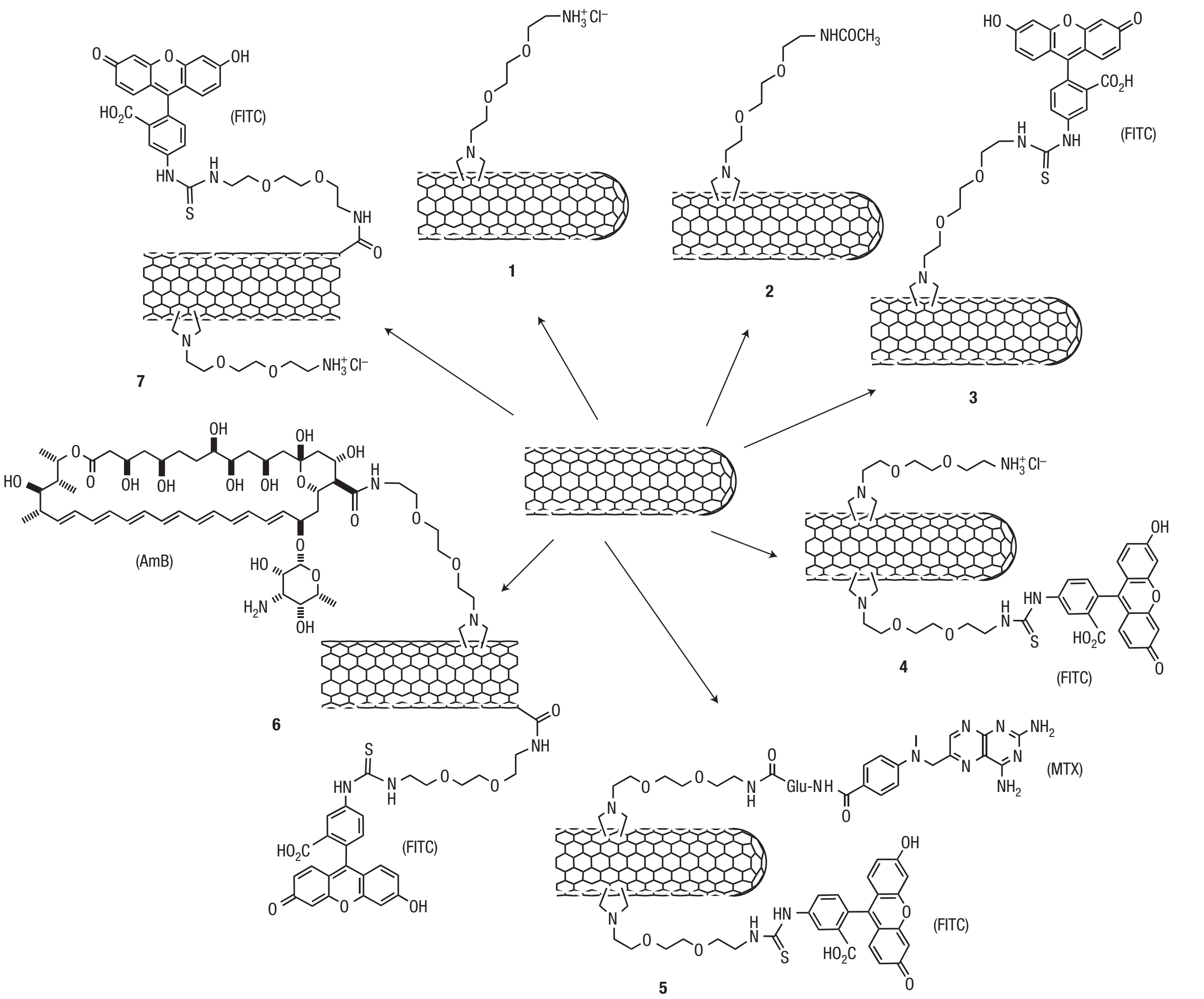

Figure 1 Molecular structures of CNT covalently functionalized with different types of small molecules. **1**, Ammonium-functionalized CNT; **2**, Acetamido-functionalized CNT; **3**, CNT functionalized with fluorescein isothiocyanate (FITC); **4**, CNT bifunctionalized with ammonium groups and FITC; **5**, CNT bifunctionalized with methotrexate (MTX) and FITC; **6**, shortened CNT bifunctionalized with amphotericin B (AmB) and FITC; **7**, shortened CNT bifunctionalized with ammonium groups and FITC (through an amide linkage).

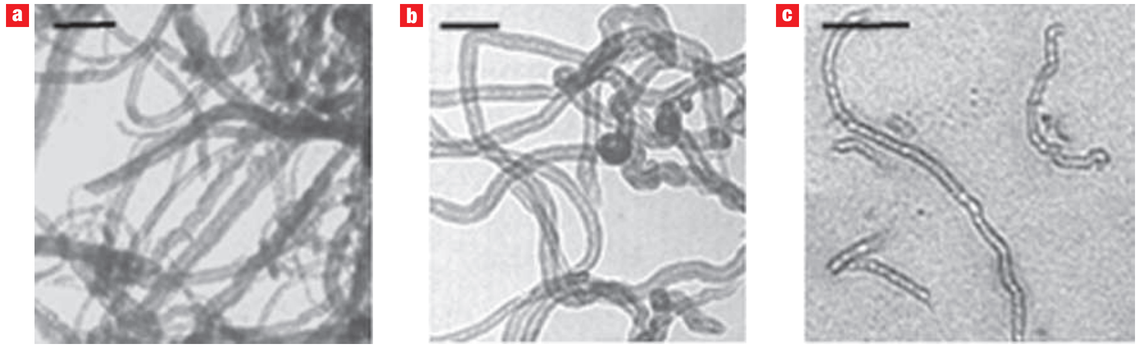

Figure 2 Structural characterization of *f*-CNTs. a–c, TEM images of pristine, non-functionalized multiwalled CNT (starting material, **a**), functionalized multiwalled *f*-CNT **1** (**b**), and functionalized multiwalled *f*-CNT **6** (**c**). The scale bar corresponds to 100 nm.

Table 1 Cellular uptake and internalization of various functionalized CNT. All studies allowed *f*-CNT (from 2 to 200 μg ml^{-1}) to interact with cells for between 1 and 4 h at 37 °C. The green signal in all images corresponds to the *f*-CNT. The nuclei of the cells incubated with *f*-CNT 1 and *f*-CNT 2 were counterstained with propidium iodide (red). The type of *f*-CNT and type of cells shown in the confocal microscopy images are highlighted in bold.

f-CNT	CNT characteristics		Cell type	Confocal microscopy images
	Type	Loading* (mmol g^{-1})		
1	***f*-SWNT** *f*-MWNT	0.45–0.55 0.85–0.95	**A549** (20 μg ml^{-1})‡ Fibroblasts HeLa CHO HEK293	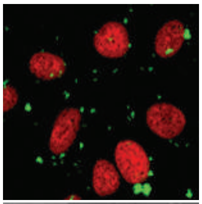
2	***f*-SWNT** *f*-MWNT	0.45–0.55 0.85–0.95	**A549** (20 μg ml^{-1})‡ Fibroblasts HeLa CHO HEK293	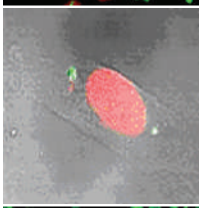
3	***f*-SWNT** *f*-MWNT	0.45–0.55 0.85–0.95	**HeLa** (2 μg ml^{-1})‡ Fibroblasts CHO HEK293 Keratinocytes A549	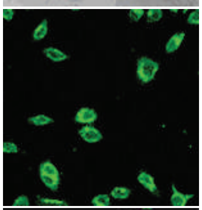
4	***f*-MWNT**	0.95 (0.65)†	**MOD-K** (5 μg ml^{-1})‡ Jurkat	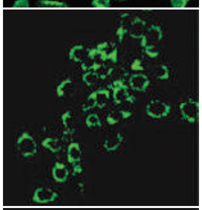
5	***f*-MWNT**	0.95 (0.65)†	**Jurkat** (5 μg ml^{-1})‡	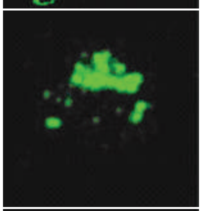
6	***f*-MWNT**	0.71 (0.25)†	**Jurkat** (20 μg ml^{-1})‡	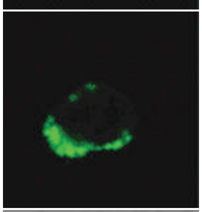
7	***f*-MWNT**	0.71 (0.25)†	***C. neoformans*** (10 μg ml^{-1})‡ *E. coli* *S. cerevisiae*	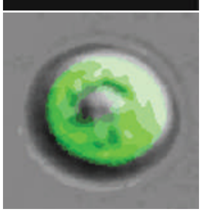

*The loading represents the total amount of functional groups (amino groups) available on the CNT surface as calculated by quantitative Kaiser test. The amino functions were then partially or completely derivatized with different active molecules.
†The number in parentheses corresponds to the amount of fluorescein linked to the amino groups. The difference from the total loading corresponds to the amount of free ammonium groups or active molecules.
‡The amount of *f*-CNT used for the internalization study associated with the particular cell type.

are shown for either *f*-SWNTs or *f*-MWNTs. The 'Cell type' column lists all the different types of cells. Representative imaging data from these studies are included following *f*-CNT (green channel signal) interaction with adherent mammalian cell monolayers (A549, HeLa, MOD-K), mammalian cell suspensions (Jurkat), fungal cells (*Cryptococcus neoformans*), yeast (*Saccharomyces cerevisiae*) and bacteria (*Escherichia coli*). Throughout these studies, *f*-CNTs seemed capable of cellular internalization in all cell types. It could be observed that the nature of the functional group on the CNT surface did not determine whether *f*-CNTs were internalized or not. Even in cases where the functional groups were electrostatically neutral (*f*-CNT **2**) or negatively charged in physiological conditions (*f*-CNT **3**), nanotubes were consistently taken up by cells.

Moreover, *f*-CNT **7** was internalized within all types of non-mammalian, prokaryotic cells as identified by confocal microscopy. Although only 20% of the *E. coli* were able to internalize the nanotubes, this was most likely due to the particularly resistant cell wall. Fluorescence was detected in 60 and 100% of *Saccharomyces cerevisiae* and *Cryptococcus neoformans*, respectively. The fact that *f*-CNTs were internalized by fungi and yeast cells (which contain a capsule composed primarily of a high molecular weight polysaccharide lacking the capability for the active energy-dependent mechanism of cellular uptake called endocytosis) was considered another indication of the observed capacity of *f*-CNTs to be taken up by all the cell types used and through the involvement of mechanisms other than endocytosis.

In an attempt to elucidate the intracellular localization of *f*-CNTs following their internalization, we allowed the interaction of single-walled *f*-CNT **1** with human alveolar epithelial (A549)

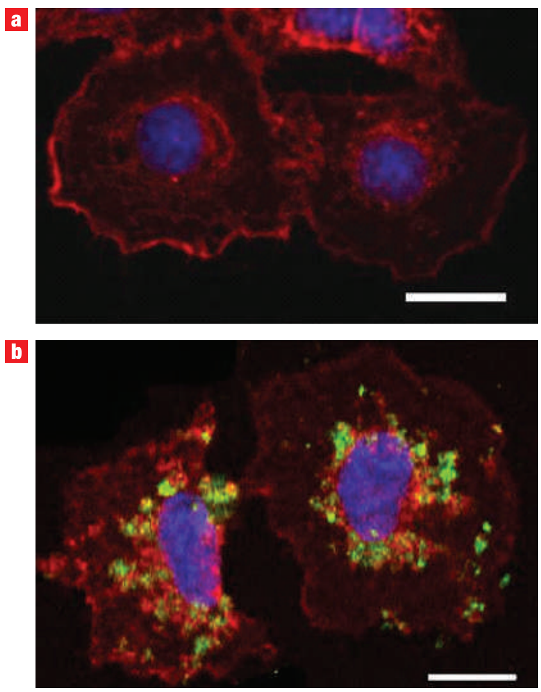

Figure 3 Intracellular trafficking and perinuclear localization of SWNT–NH_3^+ 1. a,**b**, Triple-channel confocal image of A549 cells incubated for 2 h (**a**) in the absence (control) and (**b**) with 25 μg of *f*-CNT **1** (green). Plasma membrane stained with dye WGA-TRITC (red) and nucleus counterstained with dye TO-PRO3 (blue). The scale bars corresponds to 20 μm.

cells for 2 h at 37 °C, followed by staining of the nucleus (blue) and all cellular membranes (red). The luminescence signal from the tubes (green) allowed the direct imaging of their intracellular localization using CLSM (Fig. 3). The green signal from the *f*-CNTs was distributed equally throughout the cell. The intracellular trafficking of *f*-CNT **1** led to their localization in the perinuclear region after 2 h of incubation with the cells. This observation is the first direct evidence of intracellular transport and translocation towards the cell nucleus of *f*-CNTs that have not been coated using macromolecules by fluorescence microscopy techniques. Studies using polymers or biomacromolecules coating CNTs should be considered with caution, because the presence of the macromolecules at the CNT surface will inevitably influence all interactions with cells and the intracellular transport kinetics. The perinuclear localization of *f*-CNTs shown here is an indication of the opportunities offered by nanotubes alone for intracellular delivery of therapeutics or monitoring of disease.

In order to study the influence of endocytosis-inhibiting conditions on the observed uptake and internalization of *f*-CNTs, different doses of *f*-CNTs **4**, **5** and **6** were incubated with Jurkat cells in the presence of sodium azide (NaN_3) at 4 °C—conditions commonly used to inhibit endocytosis—and analysed by epifluorescence microscopy and flow cytometry. Figure 4a depicts fluorescence-activated cell sorter (FACS) histograms for cells after 1.5 h of interaction with 5 μg ml^{-1} *f*-CNT **5**, following pretreatment of cells using different doses of NaN_3. It is clear that there is no significant shift in the fluorescence intensity of cells with and without NaN_3 treatment. This behaviour was observed also for *f*-CNT **4** and it was independent of the dose of the *f*-CNT (Fig. 4b). Jurkat cells were then allowed to interact with *f*-CNTs for up to 16 h without any major shift in the FACS signal. In addition, the cells remained alive during this long incubation time and in the presence of NaN_3. After 16 h of incubation in the presence of NaN_3, Jurkat cells were imaged using epifluorescence microscopy and obtained a strongly associated green signal from the internalized FITC-labelled *f*-CNTs (Fig. 4c, d). Finally, *f*-CNT **6** was shown to be internalized within Jurkat cells even when interaction between the nanotubes and the cells was carried out at 4 °C and in the presence of NaN_3 (Fig. 4e, f).

The data reported here indicate that cellular internalization of *f*-CNTs takes place in a wide variety of cell types, some of which exhibit deficient phagocytosis (fibroblasts) or altogether lack the machinery for endocytosis (fungi, yeast and bacteria), and even under conditions commonly used to prevent uptake of extracellular material by energy-dependent mechanisms, including endocytosis. We have previously experimentally observed that the *f*-MWNTs also used in this study can penetrate the plasma membrane of mammalian (HeLa) cells and translocate into the cytoplasm[2,7]. Even though the present study is not able to conclusively determine a single mechanism predominantly responsible for cellular uptake, it suggests that the observed cellular internalization of *f*-CNTs does not solely depend on endocytosis. Such data are in contrast to previous reports by Kam *et al.*[12,18], who, under endocytosis-inhibiting conditions, observed considerable reduction in the cellular uptake of the fluorescently labelled macromolecules used to solubilize the CNT. We believe such discrepancies are due to the sharp differences in the characteristics of the CNT constructs studied. More specifically, Kam *et al.* may well be observing strong endocytosis-dependent cellular internalization of the complexes formed between proteins[12] or single-stranded oligonucleotides and the more hydrophobic oxidized CNTs used[31]. This can be expected, as is commonly observed with supramolecular complexes formed between biological macromolecules and other nanoparticles (for example liposome–oligodeoxynucleotide, polymer–DNA).

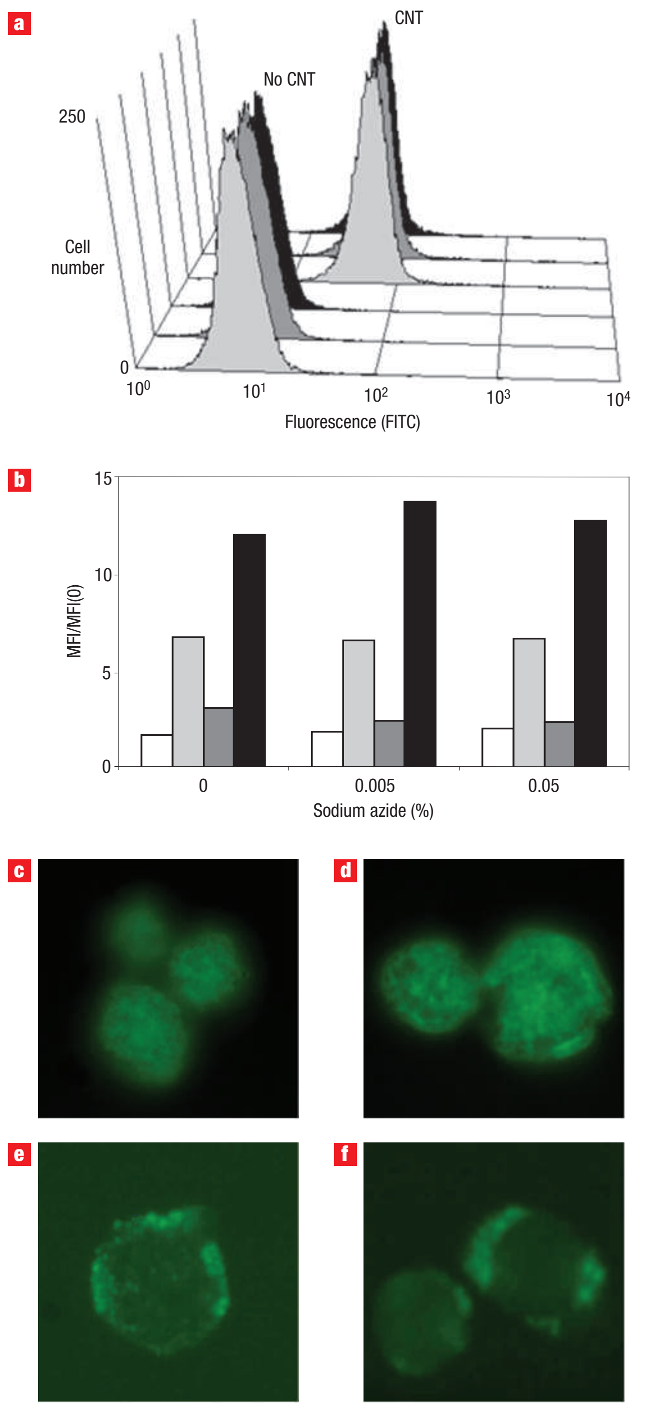

Figure 4 Internalization under endocytosis-inhibiting conditions. a, Flow cell cytometry histograms after interaction of Jurkat cells for 1.5 h at 37 °C with CNT **5** (5 μg ml^{-1}) following incubation of cells with different doses of NaN_3 in comparison to control cells treated with NaN_3 in the absence of CNTs. Light grey: 0% NaN_3; dark grey: 0.005% NaN_3; black: 0.05% NaN_3. **b**, Flow cell cytometry data showing the ratios between mean fluorescent intensity (MFI) of cells with *f*-CNTs and MFI of control cells without *f*-CNTs, MFI(0) at different doses of NaN_3. White bar: *f*-CNT **5** at 0.5 μg ml^{-1}; light grey bar: *f*-CNT **5** at 5 μg ml^{-1}; dark grey bar: *f*-CNT **4** at 0.5 μg ml^{-1}; black bar: *f*-CNT **4** at 5 μg ml^{-1}. **c**,**d**, Epifluorescence images of Jurkat cells incubated for 16 h at 37 °C (**c**) with *f*-CNT **4** (0.5 μg ml^{-1}) and (**d**) with *f*-CNT **5** (5 μg ml^{-1}) in the presence of NaN_3. **e**,**f**, Epifluorescence images of Jurkat cells incubated for 1 h with *f*-CNT **6** (20 μg ml^{-1}) (**e**) at 4 °C and (**f**) in the presence of NaN_3.

In this study the intracellular trafficking of individual or small bundles of *f*-CNTs occurred, and the transportation of nanotubes towards the perinuclear region was observed a few hours following initial contact with the cells, even under endocytosis-inhibiting conditions. Other mechanisms (such as phagocytosis)—depending on cell type, size of nanotube, extent of bundling—may also be contributing to or be triggered by the ability of *f*-CNTs to penetrate the plasma membrane, and therefore be directly involved in the intracellular trafficking of the *f*-CNTs. Overall, it can be concluded that *f*-CNTs possess a capacity to be taken up by mammalian and prokaryotic cells and to intracellularly traffic through the different cellular barriers by energy-independent mechanisms. The cylindrical shape and high aspect ratio of *f*-CNTs can allow their penetration through the plasma membrane, similar to a 'nanosyringe', as has been experimentally reported[7] and theoretically simulated[32].

METHODS

CNT

The pristine SWNTs (Carbon Nanotechnologies) used in this experiment were CNI Grade, Lot No. R0496. According to the manufacturer, the mean diameter of the SWNTs is about 1 nm. Tubes have lengths of between 300 and 1,000 nm. However, accurate SWNT length determination after functionalization is a topic of intensive current research because the dispersed tubes organize themselves into ropes. MWNTs (Nanostructured and Amorphous Materials, Lot No. 1240XH) were 94% pure, with outer diameters between 20 and 30 nm, and lengths between 0.5 and 2 μm.

FUNCTIONALIZATION OF CNTS

Amino-functionalized SWNTs and MWNT **1** were prepared as described previously[23]. Acetylated CNT **2** was obtained by simple treatment of CNT **1** with acetic anhydride in dichloromethane followed by reprecipitation in diethyl ether. FITC-labelled CNT **3** was prepared as described elsewhere[5]. Double-functionalized CNTs **4** and **5** were prepared as described earlier[25]. Double-functionalized CNTs **6** and **7** first underwent an oxidation step, which shortened the tubes and generated surface carboxylic groups that were subsequently amidated[24]. All functionalized SWNTs and MWNTs have been previously characterized using different spectroscopic and microscopic techniques. These can be found in the respective publications reporting the preparation of the material (see references).

TRANSMISSION ELECTRON MICROSCOPY

Transmission electron microscopy was performed on Hitachi H600 and Philips 208 microscopes working at different accelerating voltages and magnifications. Images were obtained using a CCD high-resolution camera AMT. The samples were prepared on 200 mesh coated copper grids with carbon–Formvar from Electron Microscopy Sciences.

CELL CULTURE

3T6, 3T3, HeLa, Jurkat human T-lymphoma and MOD-K cells (ATCC) were cultured as exponentially growing confluent monolayers on a 75-cm^2 flask in RPMI 1640 (Cambrex Bioscience) supplemented with gentamicin and 10% (v/v) heat-inactivated fetal bovine serum. Human keratinocytes (ATCC) were cultured as exponentially growing confluent monolayers on a 25 cm^2 flask in MEM (Gibco) supplemented with gentamicin and 10% (v/v) heat-inactivated fetal bovine serum. A549 cells were grown on a 75 cm^2 flask in Dulbecco's Modified Eagle Medium (D-MEM) (Gibco), CHO cells in Kaighn's Modification Medium (F12K) and HEK293 cells in Minimum Essential Medium (Eagle) (Gibco) and were supplemented with 10% fetal bovine serum (FBS) (Invitrogen) and 1% antibiotic mixture (penicillin/streptomycin) (Invitrogen). Cells were grown in suspension at 37 °C in a humidified atmosphere with 5% CO_2. *Cryptococcus neoformans* (ATCC 90112), *Saccharomyces cerevisiae* (c.i.) and *Escherichia coli* (BL21) strain cells were grown in RPMI 1640 (Cambrex Bioscience) at 37 °C in suspension with moderate shaking.

FLOW CYTOMETRY MEASUREMENTS

For the NaN_3 dose–response study, Jurkat cells (5×10^5) were initially pre-incubated at 37 °C for 0.5 h with 0%, 0.005% and 0.05% of NaN_3, respectively, before the addition of *f*-CNTs **4** and **5** (0.5 and 5 μg ml^{-1} for each *f*-CNT). After incubation for 1.5 h, cells were washed twice and resuspended with phosphate buffered saline (PBS). Cells were analysed with the flow cytometer FACSCalibur operating at 488 nm excitation wavelength and detecting emission wavelengths with a 530/30 nm bandpass filter. At least 25,000 cells were counted using the CellQuest 3.3 software (Becton & Dickinson) and distribution of the FITC fluorescence was analysed with the WinMDI 2.8 freeware (Joseph Trotter, Scripps Research Institute).

EPIFLUORESCENCE AND CONFOCAL MICROSCOPY IMAGING

Generally, cells were seeded at a density between 5×10^5 and 2×10^6 cells ml^{-1} in 2 ml of medium containing the appropriate amount of *f*-CNT (0.5–20 μg ml^{-1}). Cells were then incubated at 37 °C for 1–16 h depending on the type of *f*-CNT used. *C. neoformans, S. cerevisiae* and *E. coli* strain cells were incubated in 1 ml of PBS at room temperature, in the dark, for 1 h in the presence or not of 10 μg of *f*-CNT **7**.

Received 20 October 2006; accepted 15 December 2006; published 28 January 2007.

References

1. Martin, C. R. & Kohli, P. The emerging field of nanotube biotechnology. *Nat. Rev. Drug Discov.* **2,** 29–37 (2003).
2. Bianco, A., Kostarelos, K., Partidos, C. D. & Prato, M. Biomedical applications of functionalised carbon nanotubes. *Chem. Commun.* 571–577 (2005).
3. Lin, Y. *et al.* Advances toward bioapplications of carbon nanotubes. *J. Mater. Chem.* **14,** 527–541 (2004).
4. Bianco, A., Kostarelos, K. & Prato, M. Applications of carbon nanotubes in drug delivery. *Curr. Opin. Chem. Biol.* **9,** 674–679 (2005).
5. Pantarotto, D., Briand, J. P., Prato, M. & Bianco, A. Translocation of bioactive peptides across cell membranes by carbon nanotubes. *Chem. Commun.* 16–17 (2004).
6. Pantarotto, D. *et al.* Synthesis, structural characterization, and immunological properties of carbon nanotubes functionalized with peptides. *J. Am. Chem. Soc.* **125,** 6160–6164 (2003).
7. Pantarotto, D. *et al.* Functionalized carbon nanotubes for plasmid DNA gene delivery. *Angew. Chem. Int. Edn* **43,** 5242–5246 (2004).
8. Singh, R. *et al.* Binding and condensation of plasmid DNA onto functionalized carbon nanotubes: Toward the construction of nanotube-based gene delivery vectors. *J. Am. Chem. Soc.* **127,** 4388–4396 (2005).
9. Cai, D. *et al.* Highly efficient molecular delivery into mammalian cells using carbon nanotube spearing. *Nat. Methods* **2,** 449–454 (2005).
10. Gao, L. Z. *et al.* Carbon nanotube delivery of the GFP gene into mammalian cells. *ChemBioChem.* **7,** 239–242 (2006).
11. Liu, Y. *et al.* Polyethylenimine-grafted multiwalled carbon nanotubes for secure noncovalent immobilization and efficient delivery of DNA. *Angew. Chem. Int. Edn* **44,** 4782–4785 (2005).
12. Kam, N. W. S. & Dai, H. J. Carbon nanotubes as intracellular protein transporters: Generality and biological functionality. *J. Am. Chem. Soc.* **127,** 6021–6026 (2005).
13. Cherukuri, P., Bachilo, S., Litovsky, S. & Weisman, R. Near-infrared fluorescence microscopy of single-walled carbon nanotubes in phagocytic cells. *J. Am. Chem. Soc.* **126,** 15638–15639 (2004).
14. Heller, D., Baik, S., Eurell, T. & Strano, M. Single-walled carbon nanotube spectroscopy in live cells: Towards long-term labels and optical sensors. *Adv. Mater.* **17,** 2793–2799 (2005).
15. Sato, Y. *et al.* Influence of length on cytotoxicity of multi-walled carbon nanotubes against human acute monocytic leukemia cell line THP-1 in vitro and subcutaneous tissue of rats in vivo. *Mol. Biosyst.* **1,** 176–182 (2005).
16. Kagan, V. E. *et al.* Direct and indirect effects of single walled carbon nanotubes on RAW 264.7 macrophages: role of iron. *Toxicol. Lett.* **165,** 88–100 (2006).
17. Sayes, C. M. *et al.* Functionalization density dependence of single-walled carbon nanotubes cytotoxicity in vitro. *Toxicol. Lett.* **161,** 135–142 (2006).
18. Kam, N. W. S., Liu, Z. & Dai, H. J. Functionalization of carbon nanotubes via cleavable disulfide bonds for efficient intracellular delivery of siRNA and potent gene silencing. *J. Am. Chem. Soc.* **127,** 12492–12493 (2005).
19. Lu, Q. *et al.* RNA polymer translocation with single-walled carbon nanotubes. *Nano Lett.* **4,** 2473–2477 (2004).
20. Tsyboulski, D., Bachilo, S. & Weisman, R. Versatile visualization of individual single-walled carbon nanotubes with near-infrared fluorescence microscopy. *Nano Lett.* **5,** 975–979 (2005).
21. Kostarelos, K. & Miller, A. D. Synthetic, self-assembly ABCD nanoparticles; a structural paradigm for viable synthetic non-viral vectors. *Chem. Soc. Rev.* **34,** 970–994 (2005).
22. Georgakilas, V. *et al.* Organic functionalization of carbon nanotubes. *J. Am. Chem. Soc.* **124,** 760–761 (2002).
23. Georgakilas, V. *et al.* Amino acid functionalisation of water soluble carbon nanotubes. *Chem. Commun.* 3050–3051 (2002).
24. Wu, W. *et al.* Targeted delivery of amphotericin B to cells by using functionalized carbon nanotubes. *Angew. Chem. Int. Edn* **44,** 6358–6362 (2005).
25. Pastorin, G. *et al.* Double functionalisation of carbon nanotubes for multimodal drug delivery. *Chem. Commun.* 1182–1184 (2006).
26. Riggs, J. E., Guo, Z. X., Carroll, D. L. & Sun, Y. P. Strong luminescence of solubilized carbon nanotubes. *J. Am. Chem. Soc.* **122,** 5879–5880 (2000).
27. Banerjee, S. & Wong, S. S. Structural characterization, optical properties, and improved solubility of carbon nanotubes functionalized with Wilkinson's catalyst. *J. Am. Chem. Soc.* **124,** 8940–8948 (2002).
28. Lin, Y. *et al.* Visible luminescence of carbon nanotubes and dependence on functionalization. *J. Phys. Chem. B* **109,** 14779–14782 (2005).
29. Guldi, D. M., Holzinger, M., Hirsch, A., Georgakilas, V. & Prato, M. First comparative emission assay of single-wall carbon nanotubes—solutions and dispersions. *Chem. Commun.* 1130–1131 (2003).

30. Lacerda, L. *et al*. Luminescence of functionalised carbon nanotube as a tool to monitor bundle formation and dissociation in water: the effect of plasmid DNA complexation. *Adv. Funct. Mater.* **16,** 1839–1846 (2006).
31. Kam, N. W., Liu, Z. & Dai, H. Carbon nanotubes as intracellular transporters for proteins and DNA: an investigation of the uptake mechanism and pathway. *Angew. Chem. Int. Edn* **45,** 577–581 (2006).
32. Lopez, C. F., Nielsen, S. O., Moore, P. B. & Klein, M. L. Understanding nature's design for a nanosyringe. *Proc. Natl Acad. Sci. USA* **101,** 4431–4434 (2004).

Acknowledgements

This work was financially supported by the School of Pharmacy (University of London), CNRS, the "Agence National de la Recherche" (ANR-05-JCJC-0031-01) the NEURONANO program (NMP4-CT-2006-031847), University of Trieste and MUR (PRIN 2006, prot. 2006034372). S.G., W.W. and G.P. are grateful to CNRS and the French Ministry for Research and New Technologies for a post-doctoral fellowship (GenHomme Network 2003). L.L. wishes to thank the Portuguese Foundation for Science and Technology (FCT/MCTES) for a PhD fellowship (SFRH/BD/21845/2005). The authors wish to thank M. Benincasa and R. Gennaro for providing the fungal strains. Some of the confocal images were collected at the Microscopy Facility Platform located at the Institut de Biologie Moléculaire des Plantes (IBMP, Strasbourg, France).
Supplementary information accompanies this paper on www.nature.com/naturenanotechnology.
Correspondence and requests for materials should be addressed to K.K.

Author contributions

K.K., M.P. and A.B. conceived and designed the experiments. L.L., G.P., W.W., S.W., J.L., S.G. and D.P. performed the experiments. K.K., L.L., G.P., W.W., S.W., J.L., S.G., D.P., M.P. and A.B. analysed the data. K.K., M.P. and A.B. wrote the paper, and all the authors discussed the results and commented on the manuscript.

Competing financial interests

The authors declare that they have no competing financial interests.